

A Mechanical Testing Methodology for Metal Additive Manufacturing Processes

Sujitkumar Dongare^{*}, Todd E. Sparks⁺, Joseph Newkirk^{**} and Frank Liou^{*+}

^{*}Manufacturing Engineering

⁺Mechanical Engineering

^{**}Material Science and Engineering

Missouri University of Science and Technology, Rolla MO 65409

REVIEWED

Abstract

Most additive manufacturing processes are layer-by-layer deposition, thus its mechanical properties could be very different than those made from traditional manufacturing processes. This paper summarizes a mini-tensile testing methodology for additive manufacturing. Research concerning the tensile testing of metallic material has been conducted and test methods have been defined. It encompasses the methods for determination of yield strength, yield point elongation, tensile strength, elongation, and reduction of area. The study of positional variation and cooling-rate dependency in case of additive manufacturing proves to be expensive and time consuming with the full-size test specimens. Thus, this paper discussed a technique for testing of tensile properties using miniature sized test specimens. It covers detailed procedures for development of test specimens, actual testing set-up and the analysis of test results.

Introduction

Research concerning methods for tension testing of metallic materials has been very extensive. ASTM E-8 [1] comprises standards for different metals and it includes various test specimens' dimensions and various control methods for testing. Yongzhong Zhang *et al.* [2] has conducted such tests for characterization of laser direct deposited metallic parts. This work concentrated on laser deposited 663 copper alloy and 316L stainless steel samples. Bernd Baufeld *et al.* [3] also have contributed to this field by studying the tensile properties of Ti-6Al-4V components fabricated by shaped metal deposition. This work includes the testing of specimens for confirming the variation of tensile properties with respect to position, orientation, cooling rates and testing environment. Total length of the test specimen used was 10 mm. The standards and the previous work in the testing field have certain requirements for minimum dimensions of the test specimens. The gage length of 25 mm to 200 mm with overall length of 100 mm to 450 mm is set as standard for square cross section specimens.

Following the standard specimen dimensions is impossible in cases where available material for testing is insufficient. This happens in case of development of new materials or processes where the production of large specimens is either impossible or too expensive. For determining location-dependent properties, having a smaller specimen improves the spatial resolution of the investigation.

R. Kapoor *et al.* used 13.5mm long tensile specimens with 5.7 mm long gage length for study of the mechanical behavior of ultrafine grained AA5052 processed through different techniques [4]. Dog-bone-shaped mini-tensile specimens were also used by X. L. Shi *et al.* [5] and Z. Y. Ma *et al.* [6]. X. L. Shi synthesized ultrafine-grained Al-4Y-4Ni and Al-4Y-4Ni-0.9Fe

(at%) alloys and studied the mechanical behavior by performing uniaxial tension tests. Z. Y. Ma studied the effect of multiple-pass friction stir processing on microstructure and tensile properties of a cast aluminum-silicon alloy. X. L. Shi and Z. Y. Ma used the tensile specimens with gage length of 1.3mm and the width was 1mm. These tensile specimens were then polished to final thickness of ~0.5 mm.

The testing procedures discussed above were tested for maximum stress less than 500MPa. This paper aims at developing a testing procedure that would specifically be used for stronger aerospace materials, such as Ti-6Al-4V with expected UTS of approximately 900 MPa. It covers the information regarding specimen preparation, testing, and analysis of test result.

Fryer 5X - 45 machining center was used for the fabrication of test specimens and the actual tensile tests were run using a universal tester rated for 10Kpi load settings. The fractographs were obtained using Hitachi S - 4700 scanning electron microscope and the grain structure was studied via a Zeiss MC 63 optical microscope with a Canon Rebel XSI DSLR camera.

Specimen Design

ASTM-E8 provides standard test methods for tension testing of metallic materials. It provides guidelines for different types of specimens like plate-type specimens, sheet-type specimens, specimens for sheet, strip, flat wire and plate or specimens for wire, rod, and bar.

Considering these guidelines and the previous work in the field, sheet-type specimen with square cross section was designed for miniature tensile test. These specimens could either have wedge shaped shoulder ends for gripping or with pin ends. Considering the approximate size of the specimen, the grip section and the gripping mechanism in the universal test frames, a pin-loaded tension test design was selected. The ASTM E-8 standard allows for square cross section, pin-loaded specimens, but does not include a procedure for the size range dictated by these design constraints.

To design the dimensions of miniature specimen, various simulations were run. Different values of gage length, width of the specimen and the curve radius were tested. Stresses and deformation in the gage section and the grip section of the specimen were analyzed. The final dimensions were decided to confirm the elongation in the gage section leaving the grip section least affected. The designed miniature specimen thus had a gage length of 3.3 mm and width of 1 mm. The overall length of the specimen was 17.74 mm with the thickness of 1 mm. The gage area was nominally 1 mm by 1mm. The test set-up was designed for 2000N load ratings.

Grips were designed for this rating and hardened steel pins of 3 mm diameter were selected for the tests. Two 3 mm diameter holes were thus provided in the specimen for mounting the pins. The miniature specimens follow the same architecture as ASTM E-8 standard pin loaded, square cross section test specimen, as shown in Figure 1 except the dimensions of the specimen. Figure 2 shows the schematic representation of miniature size specimen. To consider the test to be valid, tensile failure has to be in the designed gage section. Figure 3 shows the expected post-failure condition of tensile test specimen that would confirm the validity of the test. The allowable dimensions of standard pin loaded and miniature specimens are compared in Table 1.

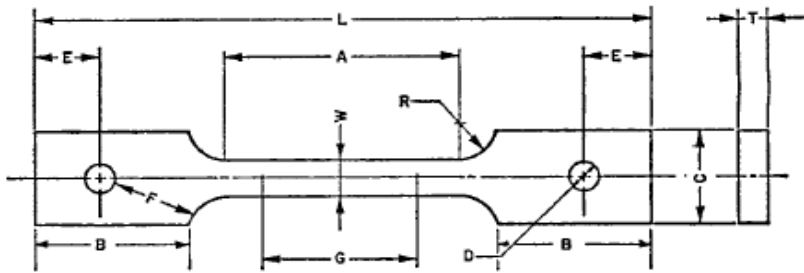


Figure 1: ASTM E8 – Sheet type pin-loaded tensile test specimen with 50mm gage length and minimum 200 mm of overall length



Figure 2: Schematic representation of designed miniature pin-loaded tensile test specimen with 3.3 mm gage length and 17.7 mm of overall length

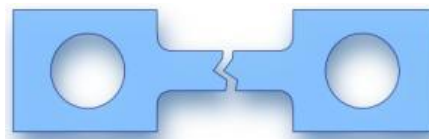


Figure 3: Expected post failure condition of designed miniature tensile specimen showing the failure in the gage section

Table 1: Comparison of dimensions of ASTM-E8 standard pin loaded specimen and designed miniature test specimen

Description	Standard pin loaded specimen dimension, mm [in.]	Miniature tensile test specimen dimension, mm
G – Gage length	50.0 ± 0.1 [2.000 ± 0.005]	3.3
W – Width	12.5 ± 0.2 [0.500 ± 0.010]	min 1
T – Thickness, max	16 [0.625]	min 1
R – Radius of fillet, min	13 [0.5]	1.25
L – Overall length	min 200 [8]	17.739
A – Length of reduced section	min 57 [2.25]	
B – Length of grip section	min 50 [2]	5.92
C – Width of grip section	approximate 50 [2]	approximate 6.05
D – Diameter of hole for pin	min 13 [0.5]	3
E – Edge distance from pin	approximate 40 [1.5]	approximate 3.02
F – Distance from hole to fillet	min 13 [0.5]	3.4

Specific grips for the miniature specimens were also designed and manufactured. The grip design consists of a 1.2 mm wide slot and a 3 mm diameter through hole for the loading pin. The test specimen placed in the slot is held together with the loading pins. Grips were machined out of 4150 steel alloy, and then heat treated to get the required hardness of approximately 42 Rockwell C. The grips were threaded for easy attachment in the universal tester. Figure 4 shows an exploded view of the test set-up.

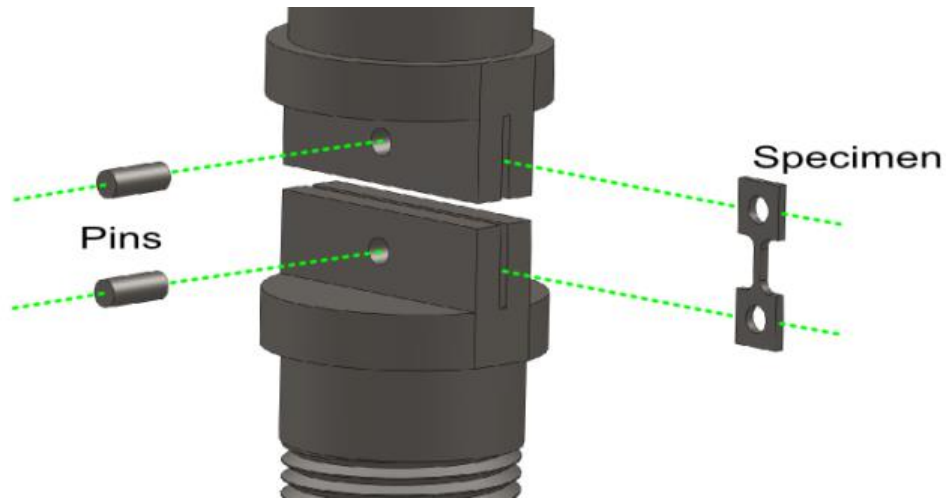


Figure 4: Exploded view of tensile test set up with newly designed miniature specimen, slotted mounting grips and the loading pins

The test set-up was designed for 2000 N force. Ti-6Al-4V specimens were expected to generate the strength of 850 – 900 MPa. For testing stronger material with this technique, testing set-up will have to be redesigned. Larger size pins would be required depending upon the expected strength value. Consequently, mounting grips and grip section of the test specimen will also need modifications to accommodate the newly confirmed loading pins.

Experimental Procedure

The experimental setup was comprised of a universal testing machine, tensile test grips, loading pins and the designed miniature test specimen. Tests were conducted as per the crosshead speed control method defined by ASTM E-8 standard. The rate of straining was set and maintained at of 0.015 ± 0.003 mm/mm/min [in./in./min] of the original reduced section. The tests were thus conducted with constant cross head speed of 0.000835 mm/s.

Specimens from wrought Ti-6Al-4V plate were first tested with this technique. Figure 5 shows the positioning of test specimens in each of the small plates. The specimens were cut from a large rolled plate of Ti-6Al-4V. It was thus expected to possess uniform properties. To test the validity of the technique, specimens generated from this plate were tested and consistent results were expected in these runs.

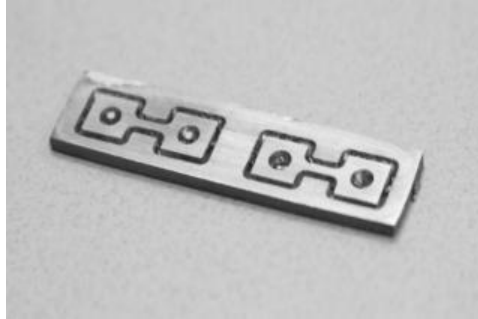


Figure 5: Positioning of miniature tensile test specimens in wrought Ti-6Al-4V plate

Having tested the specimens obtained from wrought Ti-6Al-4V plate, a few large sized laser deposits were tested using this technique. For this purpose, 45mm wide by 70 mm tall thin walls were deposited and specimens were then obtained as shown in the schematic representation in Figure 6. Next step of the experiment was to understand the ability of this technique to evaluate laser deposited structures with different cooling rates. All the deposition experiments were conducted at Laser Aided Manufacturing Processes lab (LAMP Lab) at Missouri University of Science and Technology. Ti-6Al-4V powder was supplied by Starmet Corp. and was sized at -60 +120 mesh.

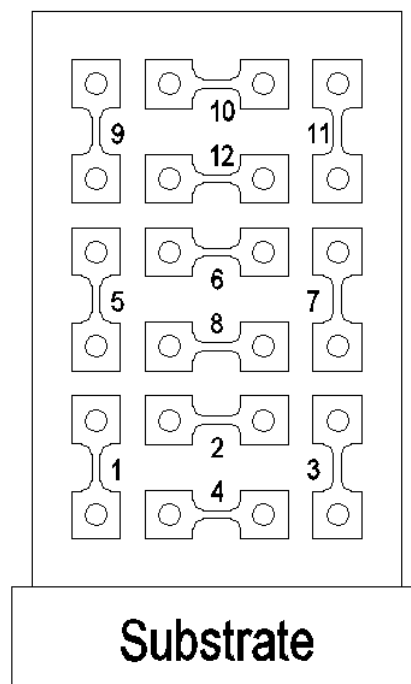


Figure 6: Schematic representation of 45mm wide by 70 mm tall deposits with positioning and orientation of the test specimens

Thin walls were deposited with the same amount of total energy and total material but with different build rates. For this purpose, the low build rate setting (375 MPPM) had laser power of 530 W with mass flow rate of 6 gm/min and travel speed of 375 mm/min. The high build rate setting (535 MPPM) used the laser power of 757 W with mass flow rate and table speed of 8 gm/min and 535 mm/min respectively. Both the settings had the same preheat conditions of two passes of 1000W and 169 layers of deposition with 45 mm travel to achieve 30 mm tall deposit. Figure 7 shows the wall deposited with 375MPPM settings and the build scheme.

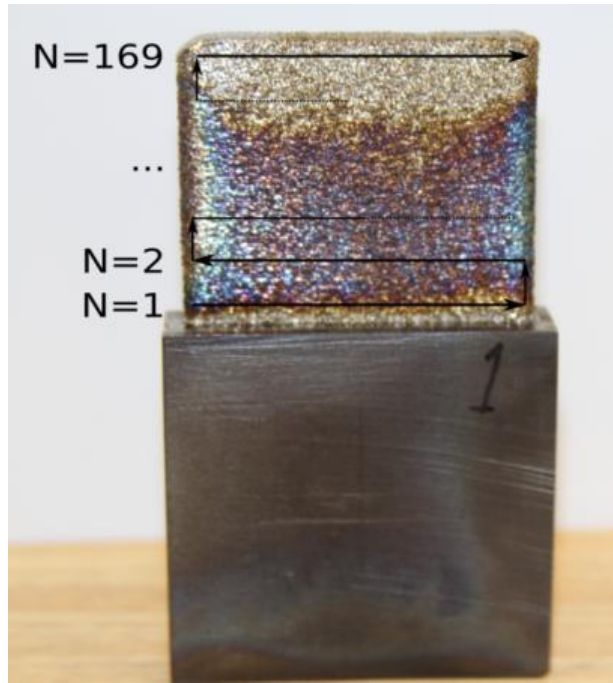


Figure 7: Ti-6Al-4V thin wall deposited with 375 MPPM setting of laser with zig-zag build scheme. Deposition started at the lower left corner. Five specimens were tested from each of such wall

A zig-zag pattern was followed for the deposition process. Two replicates were generated with each build rate setting and these are denoted with suffix A and B respectively. The number of passes being odd, the location of start and the end of the deposition process were different. Five specimens positioned as shown in Figure 8 were tested from each of these walls. To analyze the positional variation in the deposit, specimen # 1 in all the deposits was taken from the region directly above the starting point of the deposition.

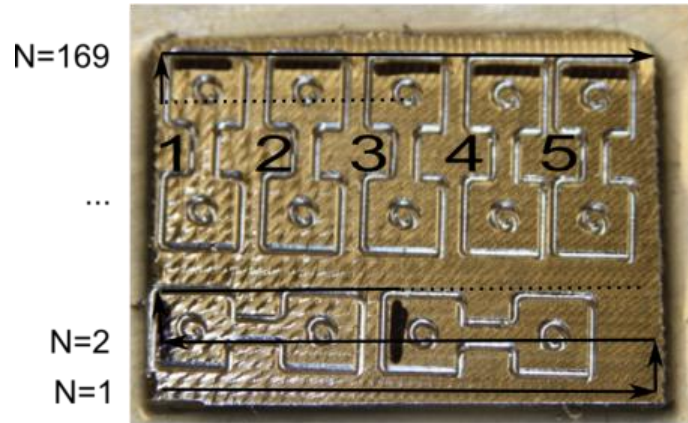


Figure 8: Positioning of miniature tensile test specimens in thin wall to test positional variation and build rate dependency. Specimen # 1 is located above the start point of deposition

Results and Discussions

Data Processing for UTS and YS Values

Force-displacement data was acquired from the test frames. Considering the original gage area, the data was plotted as stress—displacement and yield strength was further obtained. Figure 9 explains these calculations to obtain the yield strength value.

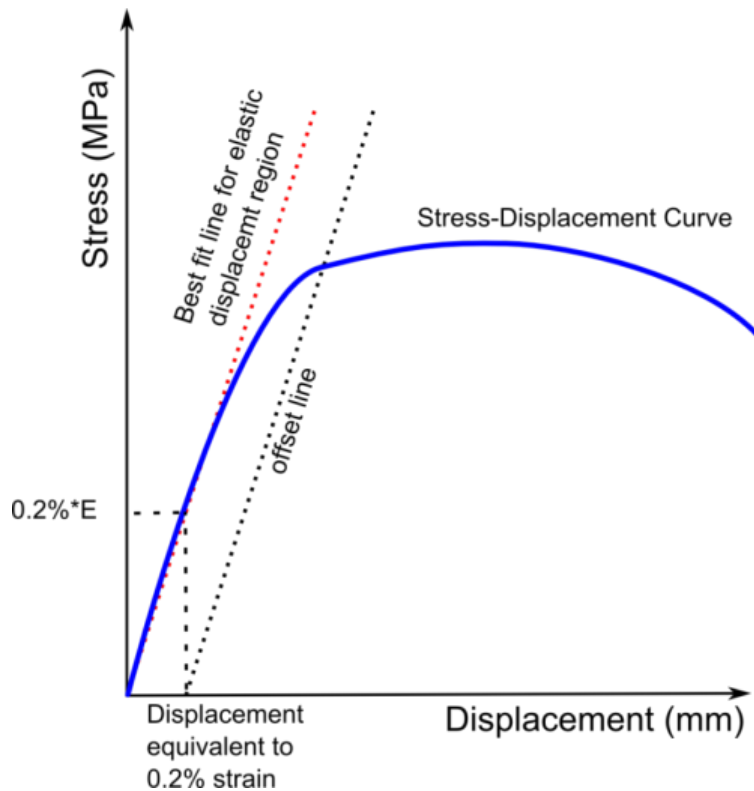


Figure 9: Schematic representation for yield strength calculation procedure using the Young's modulus value

To approximately calculate strain, the material was assumed to have constant Young's modulus value equal to 113 GPa which is the published value for annealed Ti-6Al-4V. To obtain the displacement equivalent to 0.2% strain, the 226 MPa ($113\text{GPa} * 0.002$) stress line was drawn to intersect with the stress—displacement curve. An offset line for yield strength measurement was then plotted from the x-intercept of the intersection point and parallel to the elastic portion of the curve. The point of intersection of the offset line with the actual curve Stress-Displacement curve thus provides the yield strength value. Figure 10 shows an example of the stress-displacement plot and respective values for ultimate tensile strength (UTS) and yield strength (YS).

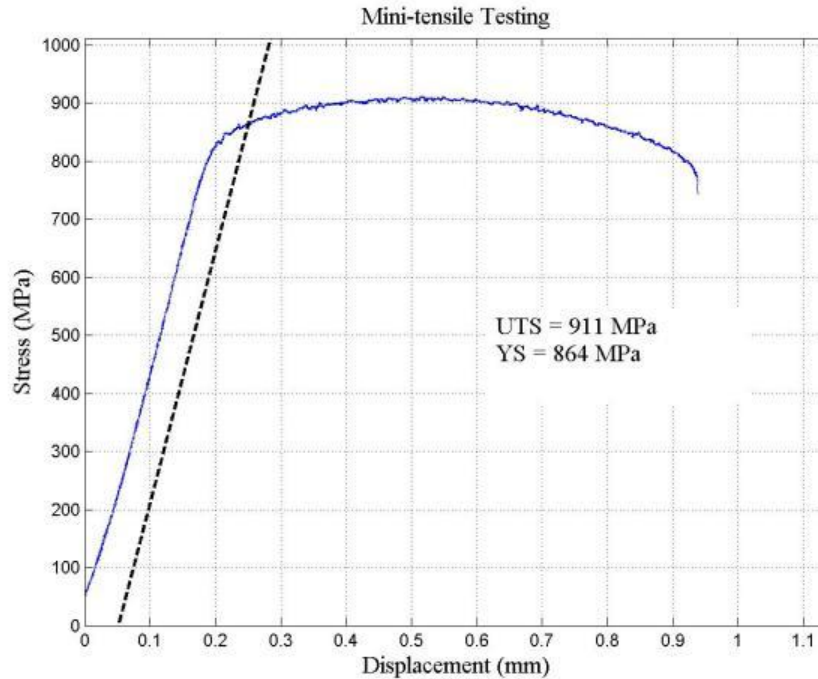


Figure 10: Example of Stress vs. Displacement plot with 0.2% offset and UTS and YS values

Testing of Wrought Ti-6Al-4V Plate

Wrought Ti-6Al-4V plate was used to understand reproducibility of the technique. Eight specimens were tested from this plate and the results were studied for mean values and variations. The detailed test results are as mentioned in Table 2. One specimen showed values out of the order with others. The results of the test were more reliable if the lowest reading was excluded. Chauvenet's criterion [7] provided a means to test the data and to determine whether a particular measurement could be removed from the data set. It was noted that this procedure allows only one measurement to be removed.

Table 2: Test results for wrought Ti-6Al-4V specimens

Sr. No.	Specimen #	UTS (MPa)	YS (MPa)	Comments
1	Specimen # 01	892	852	
2	Specimen # 02	902	870	
3	Specimen # 03	894	857	
4	Specimen # 04	911	864	
5	Specimen # 05	914	867	
6	Specimen # 06	912	869	
7	Specimen # 07	842	805	Outlier
8	Specimen # 08	923	869	

To apply Chauvenet's criterion, the arithmetic mean and standard deviation were calculated for the data set. In addition, the ratio of deviation, d_i to the standard deviation, σ was also calculated for each measurement using eq. (1) and these results are shown in Table 3 for yield strength of specimens from the wrought Ti-6Al-4V plate.

$$\frac{d_i}{\sigma} = \frac{|x_i - \bar{x}|}{\sigma} \quad (1)$$

Table 3: Yield strength data for miniature tensile test specimens from wrought Ti-6Al-4V plates to check for Chauvenet's criterion for rejecting a measurement

Specimen #	$\frac{ x_i - \bar{x} }{\sigma}$
1	0.21
2	0.61
3	0.08
4	0.34
5	0.48
6	0.57
7	2.36
8	0.57

The arithmetic mean = 856 MPa and s = 21.8 MPa.

Chauvenet's criterion requires that the ratio obtained from eq (1) must exceed a specified value before the measurement can be excluded and this value depends upon the number of tests, N. (Table 4)

According to the Table 4, the maximum deviation for the group of 8 measurements is between 1.8 and 1.96. The largest deviation in the data in Table 3 is 2.36. Chauvenet's criterion is met in case of specimen # 7 and this measurement thus can be rejected. The data was again checked for Chauvenet's criterion and the results are as shown in Table 5.

Table 4: Chauvenet's criterion for rejecting a measurement

Number of measurements, N	Ratio of maximum deviation to standard deviation, d_{\max} / σ
3	1.38
4	1.54
5	1.65
6	1.73
7	1.80
10	1.96
15	2.13
25	2.33
50	2.57
100	2.81
300	3.14

Table 5: Yield strength data for miniature tensile test specimens after rejecting a measurement

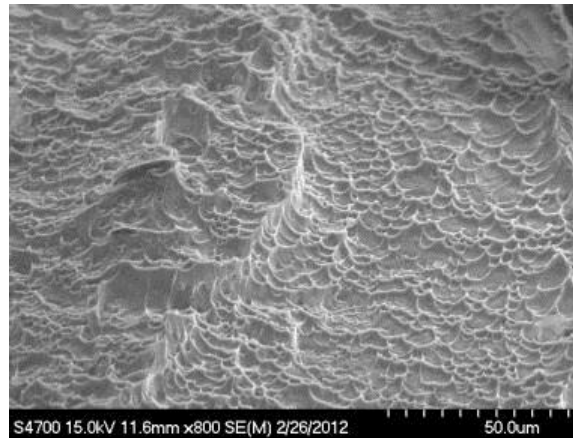
Specimen #	$\frac{ x_i - \bar{x} }{\sigma}$
1	1.73
2	0.87
3	1.01
4	0.00
5	0.43
6	0.72
8	0.72

The arithmetic mean = 864 MPa and s = 6.9 MPa.

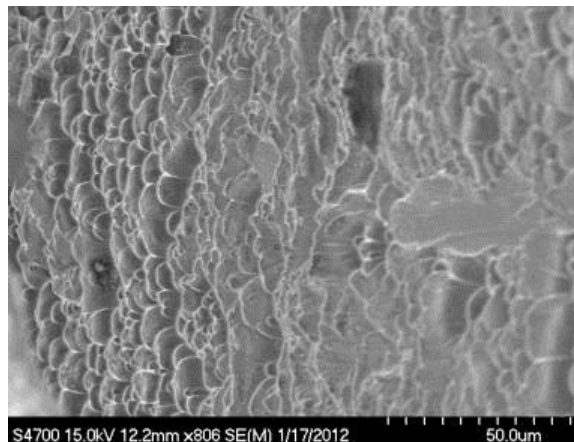
After rejecting a measurement in accordance with the Chauvenet's criterion, only seven measurements were considered for further analysis. For this data, UTS and YS was observed to be 906 ± 11 MPa, 864 ± 7 MPa respectively. These numbers are comparable with published

values [9-12] for annealed Ti-6Al-4V which is 850 – 900 MPa for UTS and 800 – 850 MPa for YS. Yield strength values obtained from miniature size specimens were also compared with the values of full size specimens obtained from different laser deposits of the same material. These specimens were horizontally oriented and were machined out of a thicker laser deposited built with different settings and conditions. Yield strengths of these specimens were 910 ± 2 MPa. Yield strength values of miniature specimens were observed to be lower but comparable with that of full size specimens. The difference in these values could be because of different build rate settings or specimen orientation. These readings help to confirm the reproducibility of the testing technique.

To investigate about the mode of fracture, fractured surfaces of test specimens were studied. Fractographs as shown in Figure 11 were obtained using a Hitachi S-4700 FESEM and were analyzed. The fractographs show dimple fracture appearance and failure was observed in the gage area which is typically a characteristic of ductile fracture. Strength numbers comparable with published values and fractographs that are evident of ductile failure confirm that this testing procedure can be considered to be reliable.



(a)



(b)

Figure 11: Fractographs of miniature tensile test specimen showing dimple fracture appearance that confirm ductile failure

Test Results from Large Size Laser Deposited Thin Walls

Having confirmed about the reproducibility of the testing technique and its results, three thin walls of the size 45mm wide by 70 mm tall were tested. 12 specimens were machined from each of these walls. Test results were as mentioned in Table 6. Specimens numbered as 2, 3, 4 and 7 from wall # 1 showed values higher than others. They will be discussed in detail later section. The rest of the specimens were observed to have mean values for UTS and YS as 912 MPa and 877 MPa respectively whereas the standard deviations for both of these were 58 MPa and 47 MPa. To investigate more about this higher standard deviation the laser deposition process was studied. This study showed that the laser deposition process was not followed as a continuous process. This had an effect on the cooling rate which ultimately affected the microstructure and the strength values. This thus confirmed the ability of the developed technique to investigate the quality of laser deposits.

Table 6: Test results for specimens from three large size walls

Specimen #	Wall # 1		Wall # 2		Wall # 3	
	UTS	YS	UTS	YS	UTS	YS
1	940	889	949	905	872	843
2	1053	1038	827	822	1000	967
3	1131	1079	908	882	882	854
4	1035	1029	893	851	904	882
5	993	944	929	905	835	814
6	834	830	900	864	937	895
7	1006	937	1073	996	957	917
8	891	891	858	851	941	894
9	909	865	921	884	969	943
10	866	828	912	856	979	919
11	949	900	820	787	961	930
12	801	719	914	883	887	875

Positional Variations in Laser Deposited Thin Walls

The ability of the testing technique to provide information regarding the positional variation in the laser deposit was studied by testing specimens from specific positions in two replicated 375 MPPM walls. UTS and YS values are tabulated in Table 7 and Figure 12 shows the distribution of YS values. Specimen # 1 denotes the area above the starting point of deposition and specimen # 5 was taken from the region closer to the end of deposition. The distribution shows that the strength values decrease from start point to the end point of deposition. In 375 MPPM A wall, lowest YS value was approximately 96 % of the highest value. This number was 91 % in case of 375 MPPM B wall. Thus the technique confirmed to investigate positional variations.

Table 7: Ultimate Tensile Strength (UTS) and Yield Strength (YS) values obtained from miniature tensile test results of two replicates of 375 MPPM walls to show the positional variation

Specimen #	373 MPPM A		373 MPPM B	
	UTS (MPa)	YS (MPa)	UTS (MPa)	YS (MPa)
1	856	821	914	884
2	862	832	871	845
3	842	821	851	822
4	883	827	824	801
5	832	796	833	805

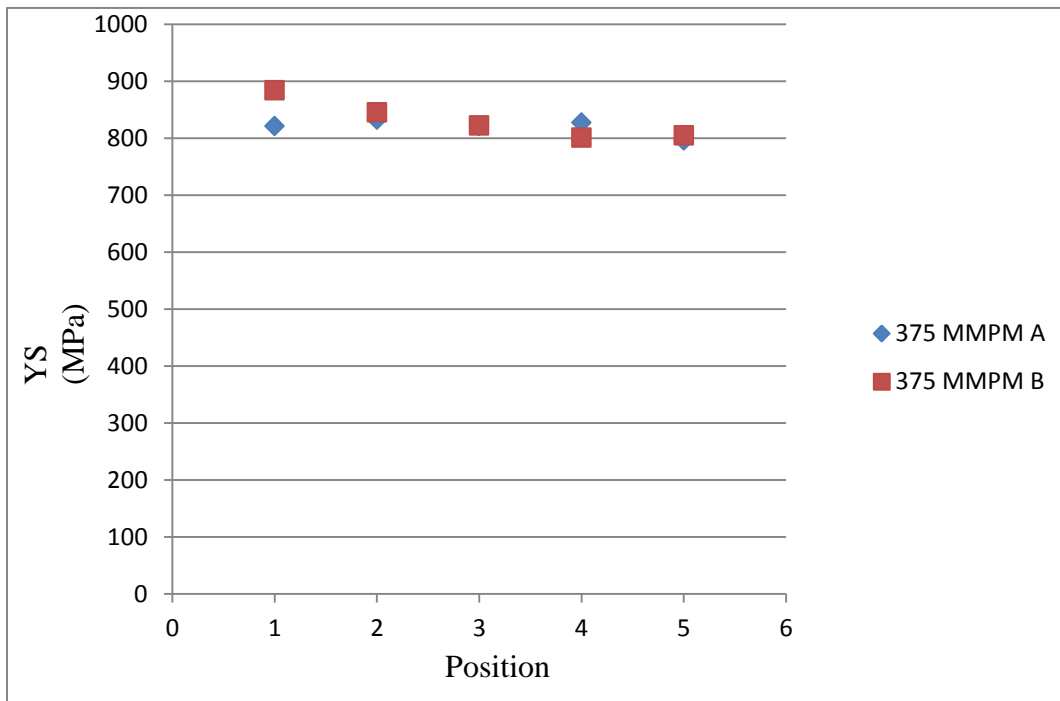


Figure 12: Distribution of miniature tensile test results from two replicates of 373 MPPM walls that shows decrease in strength values from specimen # 1 to specimen # 5. Position # 1 corresponds to the region above the start point of the build

Build Rate Dependency in Laser Deposited Thin Walls

The thin walls generated with different cooling-rates also showed interesting results. Individual readings for yield strength (YS) of specimens from 375MMPM A and 535 MMPM A walls are summarized in Table 8. The strength values were observed to have a distribution as shown in Figure 13. From the distribution it is clear that the YS value is more in case of 375 MMPM settings. The comparison of mean values of YS also has confirmed that slower build rate has produced stronger thin wall deposit.

Table 8: Yield strength values in MPa obtained from miniature tensile test results 375MMPM A and 575 MMPM A walls

Specimen #	375 MMPM A	535 MMPM A
1	821	789
2	832	820
3	821	779
4	827	795
5	796	751

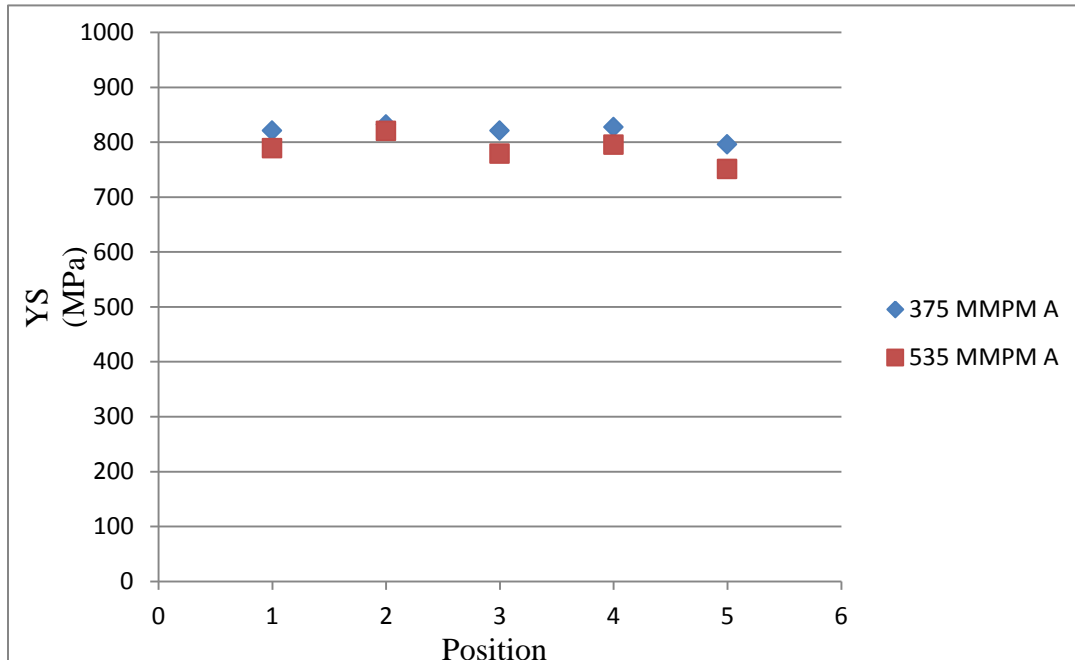


Figure 13: Distribution of miniature tensile test confirming the build rate dependency of strength values. Position # 1 corresponds to the region above the start point of the build

Effects of Large Scale Microstructure on the Technique

Reduced gage section of 1 mm by 1 mm has helped for saving the material. It should be considered that in some cases, the grains or colonies of size that is comparable to the gage section may appear in the test specimen. If these elongated micro-structures aligned with the pull direction appear to be a part of the gage section, anomalous results may be produced. Such behavior was observed in some of the specimens taken from laser deposited thin wall. The stress-displacement curve for one of such specimens is shown in Figure 14. The values for UTS and YS in such cases were observed to be exceptionally high. To investigate more about this, the grain structure in the fractured specimen was analyzed.

The fracture edge was imaged in multiple frames to form the entire edge. Two corresponding edges were as shown in Figure 15. It was seen that the grains were so arranged that three major colonies could be seen aligned in specific orientation at the fracture edge. Whereas other specimens showed Widmanstatten grain pattern as shown in Figure 16.

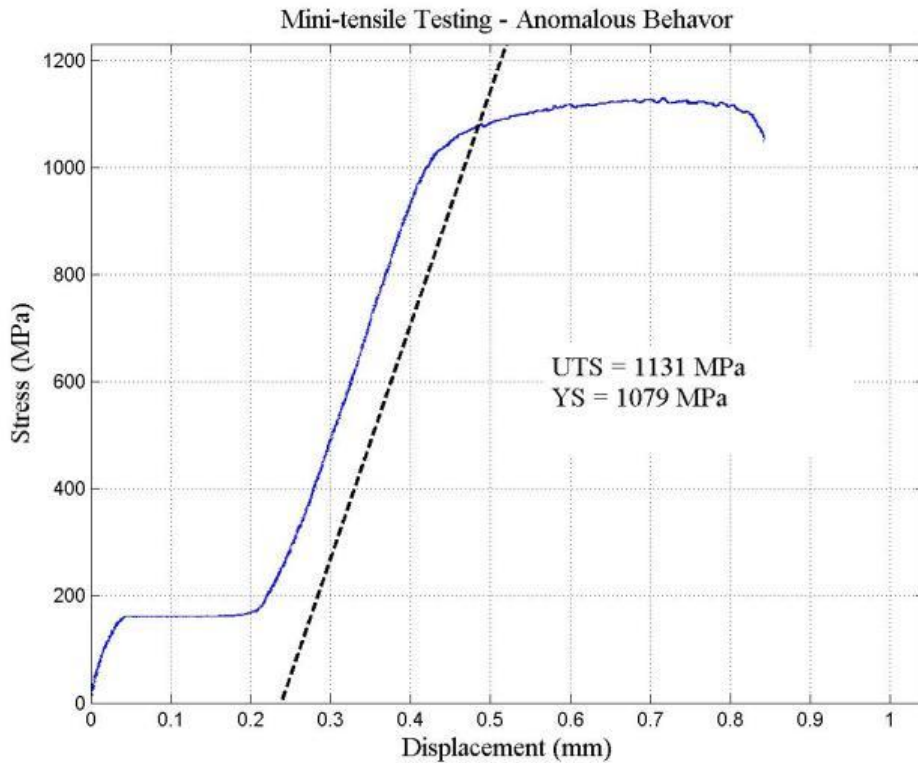
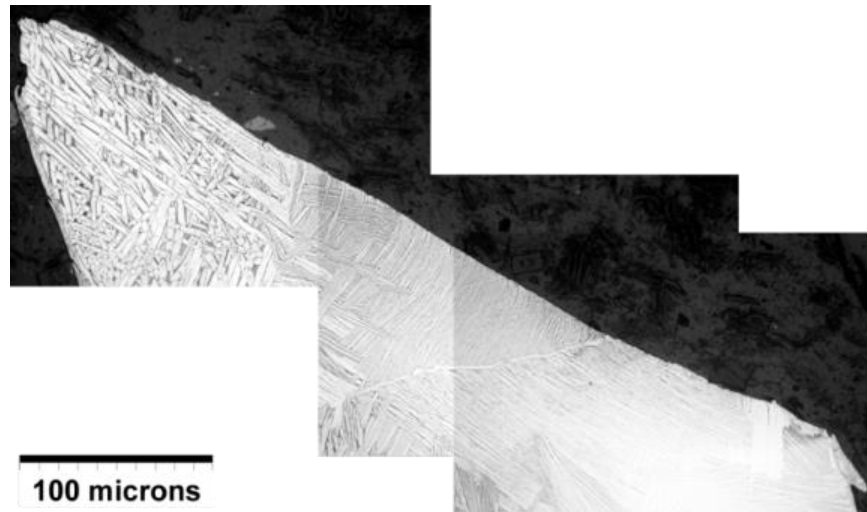
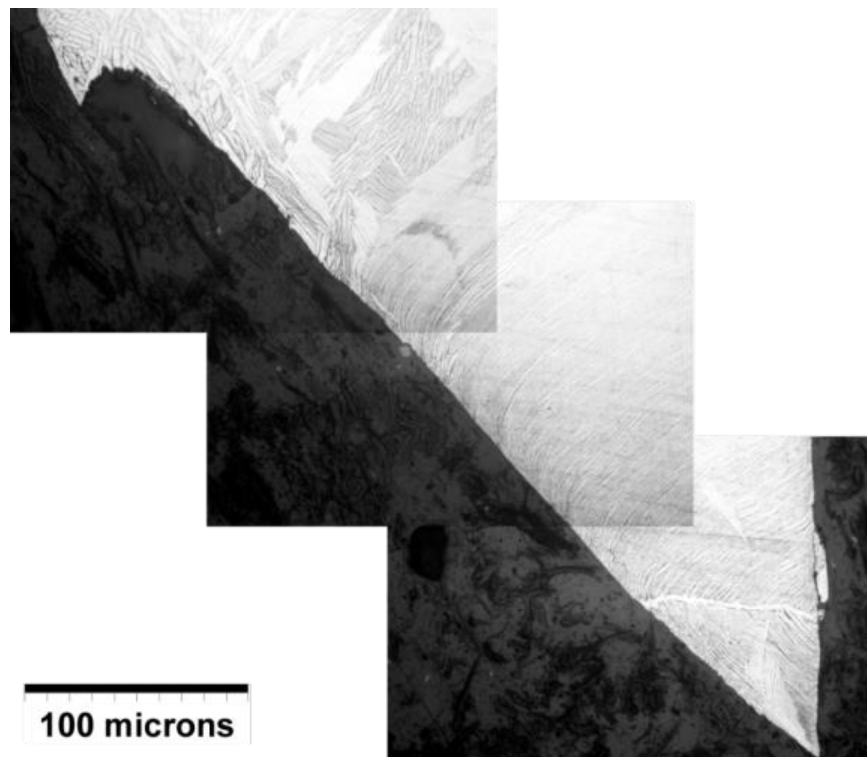


Figure 14: Stress-Displacement curve showing the anomalous behavior as a result of large size grains or colonies in the gage region

In globular grains (morphology exhibited by α phase with a mean diameter of 5 μm), main activated slip systems are prismatic ones as commonly observed in Ti alloys strained at cryogenic or room temperatures.

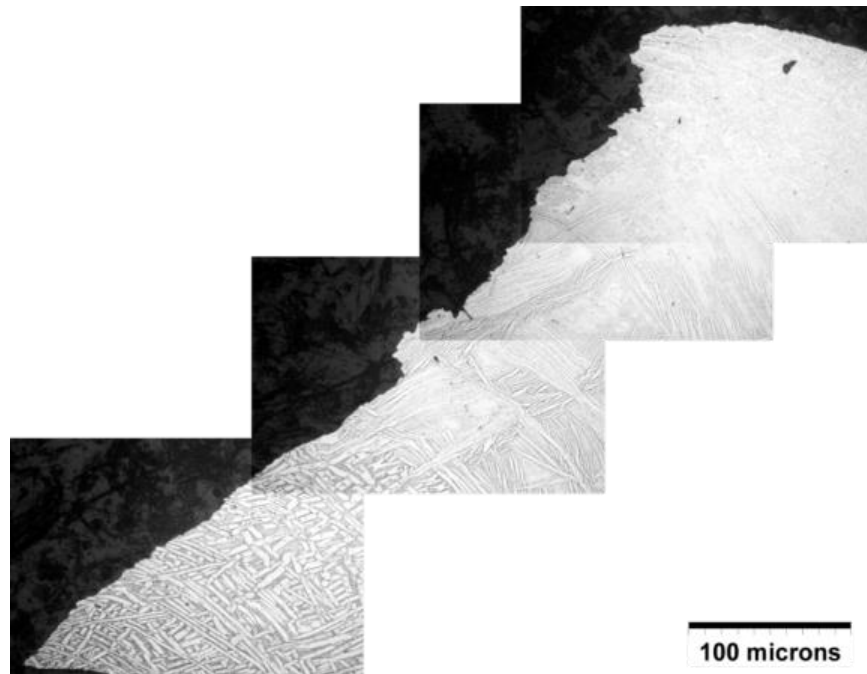


(a)

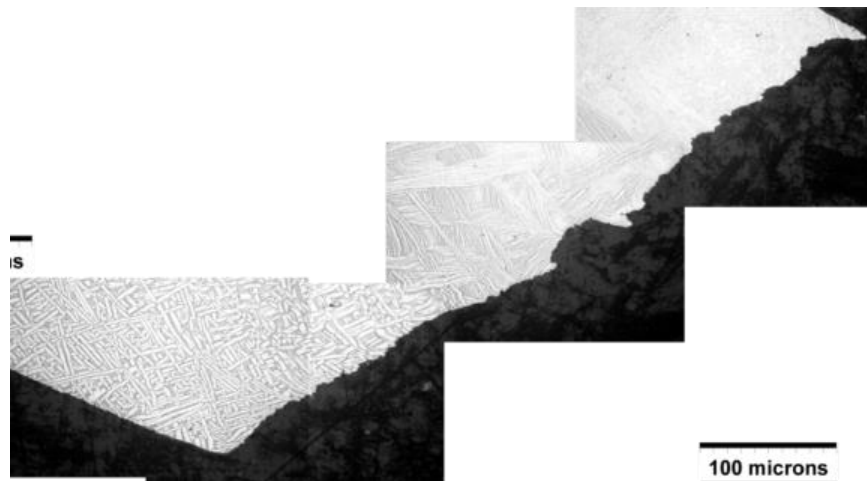


(b)

Figure 15: Optical micrographs of two fractured edges of a specimen with anomalous stress-displacement curve, showing aligned grain colonies around the fracture edge



(a)



(b)

Figure 16: Optical micrographs of two fractured edges of a specimen showing Widmanstätten grain pattern

Thus, the activation of basal systems in lath colonies does not seem to be a main deformation mode of α phase but to result from the presence of β phase lying between α laths. Due to the Burgers orientation relationship between α and β phases, some α slip systems have a correspondence in the β phase, whereas the others do not. The α/β interphases act as a filter for the α glide systems. The easy slip transmission of the basal system makes the colony size an important micro-structural parameter as compared to the α lath size.

During colonies deformation, many dislocations of the same nature pile-up against colony boundaries and produce a high stress concentration. In globular grains, the main slip system is the prismatic one, whereas in lath colonies the basal slip system is activated. This results from the presence of the β phase lying between laths in Burgers orientation relationship with the α phase. The α / β interphases act as an α glide system filter. As a consequence damage is expected to nucleate at colony boundaries. A lath colony behaves as a single grain within which the basal system only is activated. [14]

The flow curve for deformation of a single crystal of an FCC metal consists of three stages, labeled I, II, III respectively as shown in Figure 17 Stage I is that of easy glide, in which little strain hardening occurs, slip takes place on one slip system only and the dislocations move over large distances without meeting obstacles. Cottrell [15] has distinguished between two physically meaningful types of plastic flow, terming them laminar flow and turbulent flow. The former corresponds to Stage I deformation with a few long slip lines being formed and the amount of strain hardening for purely tensile or shear formation being small. The turbulent flow of Stage II corresponds to the orientation of slip on several systems, with many short slip lines formed, and the rapid strain hardening is caused by increase in internal stress from elastic interactions of these dislocations. Stage II deformation may be thought of as a stage where there is a steady increase in the number of Lomer-Cottrell barriers with increase in strain, and a consequent increase in the stress required to generate additional dislocations. Stage III deformation, with its decreasing strain hardening rate with strain, commences when dislocations are able to bypass the obstacles holding them back. The fact that strain hardening does continue is attributed to the interaction of the cross-slipped dislocations with the forest of screw dislocations which pierce the active slip planes, producing an increasing number of jogs which cannot move conservatively. Thus At higher strain, a process of dynamic recovery occurs (Stage III), where either the dislocation density decreases due to annihilation or the dislocations overcome obstacles by cross-slip [16] [18].

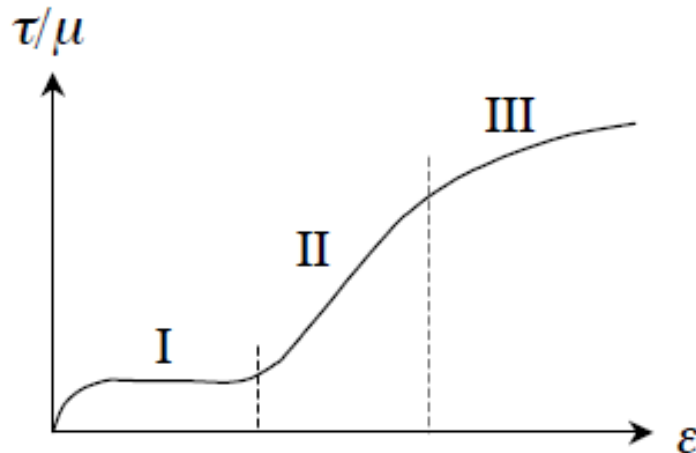


Figure 17: A typical stress-strain curve of a single crystal fcc metal at low temperature [18]

The use of this miniature size specimen tensile testing thus leaves a possibility of running into the case with larger size grain or the lath colonies behaving as a single crystal. Having such

colonies in the gage section will show higher values of UTS and YS but it should be noted that these do not necessarily correspond to the material but to the grain orientation and lath colony behavior.

Conclusion

Tensile testing procedure with miniature sized specimens was developed and tested for Ti-6Al-4V produced with different processes and settings. The specimen design is a modified version of ASTM E-8 specifications.

- The technique of testing has proven to be reliable and reproducible using wrought Ti-6Al-4V plate.
- Newly developed test set-up is capable of 2000 N force and has been successfully tested upto 1500 N.
- Technique can also be used for stronger materials following the modifications discussed in section 3.
- Yield strength values of miniature size specimens are comparable with published values and also with previously tested full size specimens.
- The procedure is also capable of confirming positional variation in strength values in a laser deposited thin wall.
- Variation induced by virtue of different build rates during laser metal deposition can also be studied using this technique. Slower build rates were observed to generate a stronger deposit.
- Tensile testing of metallic material is thus possible with saving of substantial amount of time and material with this new technique.
- The technique whereas may produce anomalous results if large grain or colonies happen to be present in the gage region.

Acknowledgments

This research was supported by U.S. Air Force Research Laboratory contract # FA8650-04-C-5704, and NASA Langley grant # NNX11AI73A. Their support is greatly appreciated.

References

- [1] ASTM, Standard E-8, “Standard Test Methods for Tension Testing of Metallic Materials” Active Standard ASTM E8 / E8M | Developed by Subcommittee: E28.04: <http://enterprise2.astm.org/DOWNLOAD/E8.143144-1.pdf>
- [2] Yongzhong Zhang, Mingzhe Xi, Shiyu Gao, Likai Shi, “Characterization of laser direct deposited metallic parts” Journal of Materials Processing Technology 142 (2003) 582–585
- [3] Bernd Baufeld and Omer van der Biest, “Mechanical properties of Ti-6Al-4V specimens produced by shaped metal deposition” Sci. Technol. Adv. Mater. 10 (2009) 015008 (10pp).

- [4] R. Kapoor, N. Kumar, R.S. Mishra, C. S. Huskamp, K. K. Sankaran, “Influence of fraction of high angle boundaries on the mechanical behavior of an ultrafine grained Al-Mg alloy”, *Materials Science and Engineering: A*, Volume 527, Issue 20, 25 July 2010, Pages 5246–5254.
- [5] X.L. Shi, R.S. Mishra, T.J. Watson, “Effect of temperature and strain rate on tensile behavior of ultrafine-grained aluminum alloys”, *Materials Science and Engineering: A*, Volume 494, Issues 1–2, 25 October 2008, Pages 247–252.
- [6] Z.Y. Maa, S.R. Sharmab, R.S. Mishra, “Effect of multiple-pass friction stir processing on microstructure and tensile properties of a cast aluminum-silicon alloy”, *Scripta Materialia* 54 (2006) 1623-1626.
- [7] J. P. Holman, *Experimental Methods for Engineers*, McGraw-Hill Book co. (5th ed.), p.63 (1989).
- [8] Tiley Jaimie, “Modeling of microstructure property relationship in Ti-6Al-4V”, 2003, Doctor of Philosophy dissertation, Ohio State University.
- [9] Maryland Metrics: Titanium Ti-6Al-4V Grade 5 (R56400) Specifications, Maryland Metrics, url: <http://mdmetric.com/tech/ti6Al-4V.htm>, date accessed: 06/08/2012.
- [10] Technical Data Ti-6Al-4V (Ti-6-4), North American Alloys, url: <http://www.northamericanalloys.com/Ti-6-4%20props.htm>, date accessed: 06/08/2012.
- [11] Titanium Ti-6Al-4V (Grade 5), STA, ASM, Aerospace Specification Metals, Inc. url: <http://asm.matweb.com/search/SpecificMaterial.asp?bassnum=MTP642>, date accessed: 06/08/2012.
- [12] Alloy Data: Titanium Alloy Ti 6Al-4V, Veridiam, url: <http://www.veridiam.com/pdf/DataSheetTitaniumAlloy.pdf>, date accessed: 06/08/2012.
- [13] S. Naka, L. P. Kubin, C. Perrier, “The plasticity of Titanium at low and medium temperatures”, *Philosophical Magazine A - Volume 63*.
- [14] A. Ambard, L. Guetaz, F. Louchet, D. Guichard, “Role of interphases in the deformation mechanisms of an titanium alloy at 20 K” *Materials Science and Engineering A319–321* (2001) 404–408.
- [15] A. H. Cottrell, “Dislocations and plastic flow in crystals, Clarendon press, Oxford (1953).
- [16] Iain LeMay, “Principles of Mechanical Metallurgy”, Elsevier, 1980.
- [17] Yaxin Bao, Mechanical properties and microstructure study for direct metal deposition of Titanium alloy and tool steel, MS thesis, University of Missouri, Rolla, 2007.
- [18] Denis Yau Wai Yu, “Microtensile Testing of Free-standing and Supported Metallic Thin Films”, Harvard University, Doctor of Philosophy dissertation, 2003.